High Temperature Studies of 140 nm T-gate AlGaN/GaN HEMT Devices

Ahmad E. Islam,[1] Adam Miesle,[2] Nicholas P. Sepelak,[2] Hanwool Lee,[3] Dennis E. Walker Jr.,[1] Nicholas C. Miller,[1] Matt Grupen,[1] Kyle J. Liddy,[1] Antonio Crespo,[1] Gary Hughes,[1] Wenjuan Zhu,[3] Kelson D. Chabak[1], and Andrew J. Green[1]

[1]Air Force Research Laboratory, Sensors Directorate, Wright-Patterson AFB, Dayton, OH 45433, USA
[2]KBR, Inc., Beavercreek, OH 45431 USA
[3]Department of Electrical and Computer Engineering, University of Illinois, Urbana, IL 61801, USA
Email: ahmad.islam.2@us.af.mil, ahmad.islam.2@afrl.af.mil

Keywords: high temperature; AlGaN/GaN HEMT; 140nm; T-gate; leakage; transconductance; reliability.

Abstract

We studied high temperature (up to 500 ºC) operation of AlGaN/GaN HEMT made using AFRL's GaN 140 nm T-gate process technology. Higher temperature measurements showed a reduction in gate modulation of the drain current. Devices also exhibited reduction in transconductance, a reduction in threshold voltage, and an increase in on-state resistance at 500 ºC, when the data was compared with room temperature measurements. During reliability characterization, devices exhibited continuous loss of gate modulation when they were measured at 400-500 ºC over time. The reliability data collected at high stress levels revealed eventual failure of these devices potentially due to diffusion of different atoms within the device.

INTRODUCTION

RF communication at high-temperature (HT) is critical for hypersonic vehicles, space exploration, and in energy-dense systems [1, 2]. These HT applications are constrained in terms of the availability of active cooling systems [2] and the requirements of decreased size, weight, power and cost (SWaP-C). Wide bandgap (WBG) materials based on III-N compounds are considered for these applications [3-5], as they have high melting points, low intrinsic carrier concentration, high breakdown electric fields. In this work, we studied room temperature to 500 ºC DC operation of AFRL's 140 nm T-gate AlGaN/GaN HEMTs.

DEVICE DETAILS

Devices were fabricated using AFRL GaN140 nm device process technology on 4" 6H-SiC substrates [6]. Devices were fabricated in mesa isolated regions using ohmic source/drain contacts made using 850 ºC annealed Ti/Al/Ni/Au in photo-lithographically defined regions spaced by L_{SD} ~ 3 µm. The T-shaped Schottky gate contact on the channel area with gate length ~ 140 nm and head spanning ~ 770 nm was defined using e-beam lithography and using Ni/Au metal layers. The devices were passivated with ~ 200 nm SiN_x and used source-connected posts with Au air bridges. Fig. 1 shows cross-sectional scanning electron microscopy (SEM) image of a device imaged after T-gate formation.

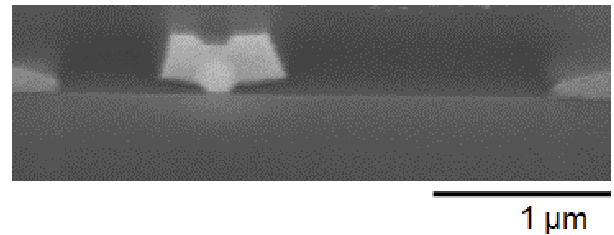

Fig. 1. Cross-sectional SEM of an AlGaN/GaN T-gate HEMT device with gate length ~ 140 nm and source-drain length ~ 3 µm. The image has been taken before SiN_x passivation of the device.

RESULTS AND DISCUSSION

Fig. 2 shows representative transfer (i.e. drain current I_D vs gate-to-source voltage V_{GS}) and output (I_D vs drain-to-source voltage V_{DS}) characteristics of a device measured at room temperature (RT). The devices exhibited a maximum to minimum drain current ratio (I_{MAX}/I_{MIN}) of ~ 10^4 at different V_{DS} (Fig. 2a), a threshold voltage V_T of ~ -3V (measured at V_{DS} = 0.1 V), maximum transconductance ($g_{m,max}$) of ~ 120 mS/mm (measured at V_{DS} = 0.1 V) and on-resistance (R_{on}) of ~ 1.5 Ω-mm.

DISTRIBUTION STATEMENT A. Approved for public release: distribution unlimited. #AFRL-2023-0241.

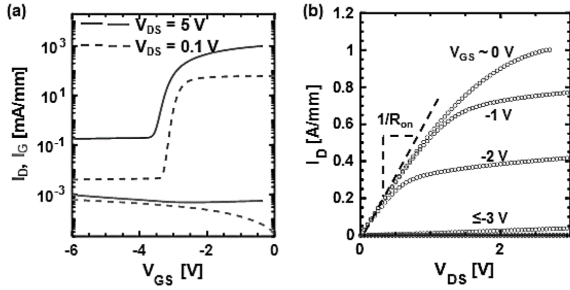

Fig. 2. I_D and I_G for an AlGaN/GaN HEMT as a function of V_{GS} measured at room temperature using V_{DS} = 0.1 V and 5 V. (b) Output characteristics (I_D vs. V_{DS}) of the same device measured at different V_{GS}. The dashed line shows the slope near V_{DS} = 0 used to calculate the on-resistance R_{on} at V_{GS} = 0V.

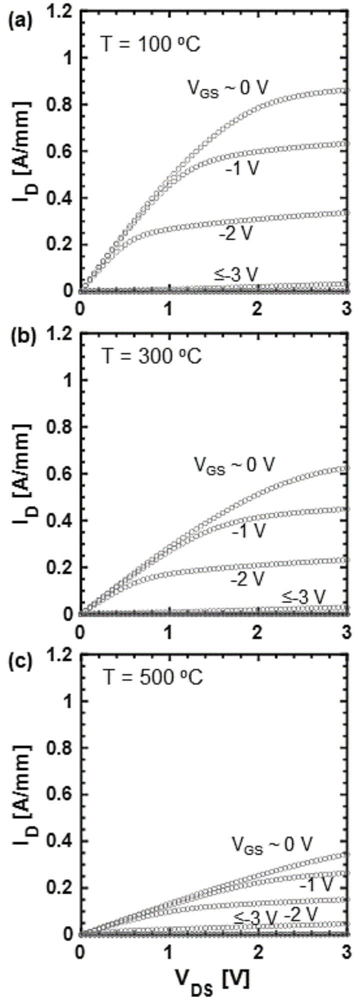

Fig. 3. Output (I_D-V_{DS}) characteristics of a device measured in vacuum using V_{GS} = -6 to 0V at temperature, T = 100 ºC, 300 ºC, 500 ºC.

The HT measurements were performed in DC using a test station from MicroXact, Inc. in vacuum. Fig. 3 shows the output characteristics of a device measured at different temperatures exhibiting a reduction in current carrying capacity by ~ 60%, when measured at V_{DS} = 3V and V_{GS} = 0V. R_{on} increased by 5 times due to the increase in sheet resistance of the 2DEG layer. This was confirmed using sheet resistance measurements in TLM test structures at different temperature, which also revealed negligible change in resistance of the source/drain contacts.

To understand the mechanism of current reduction in the devices, we compared the transfer characteristics (see Fig. 4a) measured at different temperatures and obtained different device parameters (see Figs. 4b-e). In addition to the reduction in I_{MAX}/I_{MIN} (Fig. 4b), we observed a reduction in V_T (Fig. 4c) due to the increase in off-state leakage from the flow of energetic carriers across the source-channel energy barrier.

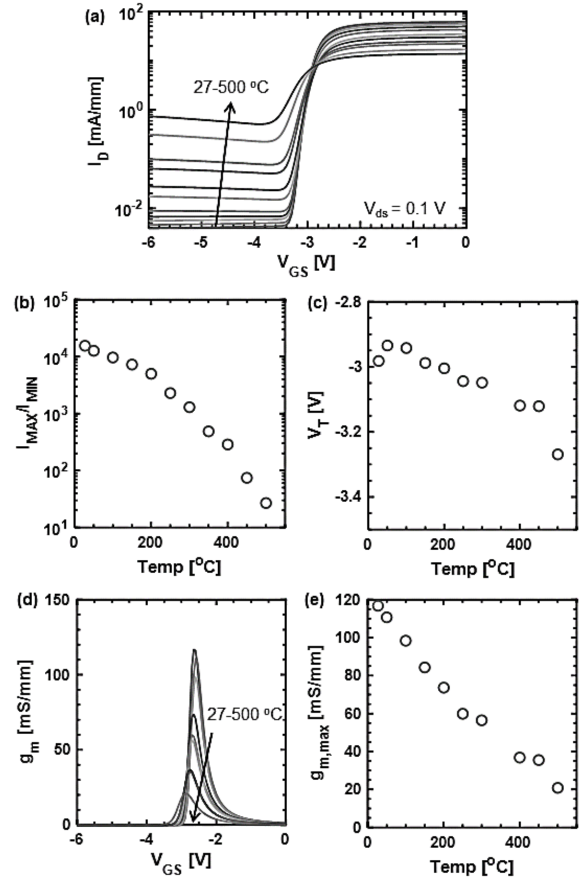

Fig. 4. (a) Transfer (I_D-V_{GS}) characteristics of a device measured at temperature T = 27, 50, 100, 150, 200, 250, 300, 350, 400, 450, 500 ºC in vacuum using V_{DS} = 0.1 V. (b-c) The variations in maximum to minimum current ratio (I_{MAX}/I_{MIN}) and threshold voltage (V_T) with temperature. (d-e) Transconductance (g_m) vs V_{GS} characteristics measured at different temperatures and variation in maximum g_m ($g_{m,max}$) with temperature.

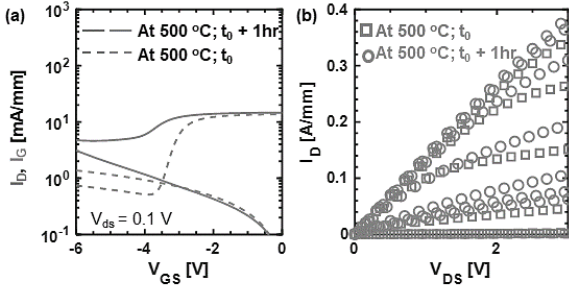

Fig. 5. (a) Transfer characteristics and gate leakage of a device measured at t_o (dashed line: right after the device was heated to 500 °C) and at ~ 1 hr after t_o (solid line). (b) Output characteristics of the device after the device was kept at 500 °C for an hour.

The g_m vs V_{GS} characteristics measured at different temperatures (Fig. 4d) showed a ~ 85% reduction in $g_{m,max}$ (Fig. 4d) due to enhanced phonon scattering with the increase in temperature.

We additionally studied the stability of the devices at 400-500 °C by measuring them intermittently and continuously (Figs. 5-6 show the 500 °C stress data only) at a fixed V_{DS} and V_{GS}. Fig. 5 revealed significant reduction in I_{MAX}/I_{MIN} for a device, when the device was kept at 500 °C for an hour. During a similar reliability testing at 400 °C, the devices also

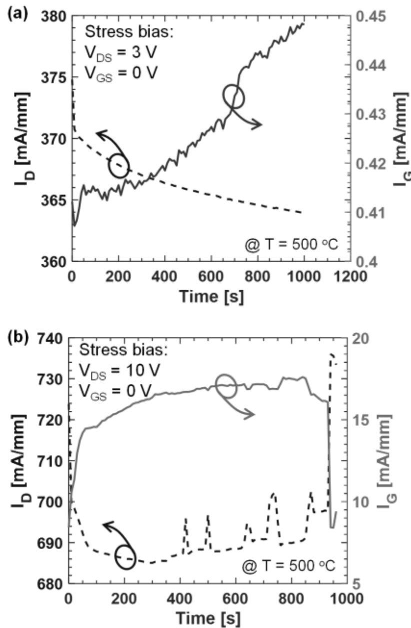

Fig. 6. Time dependent degradation of different devices stressed at T = 500 °C using (a) V_{DS} = 3V, V_{GS} = 0V and (b) V_{DS} = 10V, V_{GS} = 0V. At low V_{DS}, devices exhibited a ~ 3% reduction in I_D and a small increase in gate leakage. At higher V_{DS}, devices broke down within ~15 minutes.

showed similar degradation over time but at a slower rate. Such degradation occurred due to the increase in gate leakage in the device, which was also observed during continuous current measurements in Fig. 6. This increase in gate leakage is presumably due to the gate metal reordering and diffusion of Au into barrier layer [3]. In addition to the increase in gate leakage, devices also exhibited a ~ 3% reduction in I_D (Fig. 6a) due to increase in its contact resistance and some devices had a breakdown within ~15 minutes (Fig. 6b) when they were stressed continuously at a higher V_{DS} (= 10V) at 500 °C.

Conclusions

High temperature studies in AFRL's 140nm T-gate AlGaN/GaN HEMT devices revealed a reduction in gate modulation, threshold voltage, an approximately 85% reduction in transconductance, and an increase in on-state resistance, as devices were tested from 27 °C to 500 °C. Device reliability measurements showed continuous loss of gate modulation when they were measured at 400-500 °C over time. The reliability data collected at 500 °C and at high bias levels revealed eventual failure of these devices. The reliability of these devices can potentially be improved by engineering the gate metal structures, which will enable the application of these devices at high temperatures.

Acknowledgements

The authors would like to acknowledge financial supports from AFRL.

Acronyms

HEMT: High electron mobility transistors
AFRL: Air Force Research Laboratory
TLM: Transfer length method

References

[1] Watson *et al.*, *J. Materials Science: Materials in Electronics,* pp. 9226-9235, 2015.

[2] Neudeck *et al.*, *Proceedings of the IEEE,* pp. 1065-1076, 2002.

[3] Carey *et al.*, *IEEE J. Electron Devices Society,* pp. 444-452, 2019.

[4] Hiroki *et al.*, *IEEE Electron Device Letters,* pp. 350-353, 2022.

[5] Potts *et al.*, *IEEE Trans. Electron Devices,* pp. 4278-4282, 2021.

[6] Fitch *et al.*, *IEEE Electron Device Letters,* pp. 1004-1007, 2015.